Analytical and Bioanalytical Chemistry (2022) 414:399–412
https://doi.org/10.1007/s00216-021-03240-8

RESEARCH PAPER

Anticipating metastasis through electrochemical immunosensing of tumor hypoxia biomarkers

Cristina Muñoz-San Martín[1] · Maria Gamella[1] · María Pedrero[1] · Ana Montero-Calle[2] · Víctor Pérez-Ginés[1] · Jordi Camps[3] · Meritxell Arenas[3] · Rodrigo Barderas[2] · José M. Pingarrón[1] · Susana Campuzano[1]

Received: 2 February 2021 / Revised: 16 February 2021 / Accepted: 17 February 2021 / Published online: 26 February 2021

Abstract

Metastasis is responsible for about 90% of cancer-associated deaths. In the context of solid tumors, the low oxygen concentration in the tumor microenvironment (hypoxia) is one of the key factors contributing to metastasis. Tumor cells adapt to these conditions by overexpressing certain proteins such as programmed death ligand 1 (PD-L1) and hypoxia-inducible factor 1 alpha (HIF-1α). However, the determination of these tumor hypoxia markers that can be used to follow-up tumor progression and improve the efficiency of therapies has been scarcely addressed using electrochemical biosensors. In this work, we report the first electrochemical bioplatform for the determination of PD-L1 as well as the first one allowing its simultaneous determination with HIF-1α. The target proteins were captured and enzymatically labeled on magnetic microbeads and amperometric detection was undertaken on the surface of screen-printed dual carbon electrodes using the hydrogen peroxide/peroxidase/hydroquinone system. Sandwich immunoassays were implemented for both the HIF-1α and PD-L1 sensors and the analytical characteristics were evaluated providing LOD values of 86 and 279 pg mL^{-1} for the amperometric determination of PD-L1 and HIF-1α standards, respectively. The developed electrochemical immunoplatforms are competitive versus the only electrochemical immunosensor reported for the determination of HIF-1α and the "gold standard" ELISA methodology for the single determination of both proteins in terms of assay time, compatibility with the simultaneous determination of both proteins making their use suitable for untrained users at the point of attention. The dual amperometric immunosensor was applied to the simultaneous determination of HIF-1α and PD-L1 in cancer cell lysates. The analyses lasted only 2 h and just 0.5 μg of the sample was required.

Keywords PD-L1 · HIF-1α · Amperometry · Dual immunosensor · Tumor hypoxia · Cell lysates

Introduction

As it is known, cancer is the second cause of death in Europe and the United States after cardiovascular diseases. According to the International Agency for Research on Cancer (IARC), in 2020 about 19.3 million new cases were registered worldwide, causing 10.0 million deaths [1]. The main reason for this fatal outcome is the development of metastasis. This condition is characterized by the uncontrolled growth of cells that make up the body's tissues. In the tumor microenvironment, the limitation of oxygen and nutrients makes it necessary to form a new network of blood vessels that deliver the required supplements to the cells and eliminate the produced waste. This process, called angiogenesis, gives cancer cells the ability to migrate to other organs of the body through the newly formed vascular network, increasing their metastatic potential. Therefore, it can be said that the low oxygen concentration in the tumor microenvironment, also called hypoxia, is related to the development of metastasis and poor survival [2]. Tumor cells adapt to these hypoxic conditions by overexpressing certain proteins such as programmed death ligand 1 (PD-L1) and

Published in the topical collection celebrating *ABCs 20th Anniversary*.

✉ Susana Campuzano
susanacr@quim.ucm.es

[1] Departamento de Química Analítica, Facultad de CC. Químicas, Universidad Complutense de Madrid, 28040 Madrid, Spain

[2] UFIEC, Instituto de Salud Carlos III, 28220 Majadahonda, Madrid, Spain

[3] Unitat de Recerca Biomèdica, Hospital Universitari Sant Joan, Institut d'Investigació Sanitària Pere Virgili, Universitat Rovirai Virgili, 43204 Reus, Spain

hypoxia-inducible factor 1α (HIF-1α). In fact, a correlation has been found between PD-L1 and HIF-1α levels in cancer cells exposed to hypoxia, HIF-1α regulating PD-L1 in hypoxic environments when it interacts with a hypoxia response element of the *PD-L1* promoter to activate its transcription in cancer cell lines [3–7]. Moreover, a correlation among these two protein levels has been reported for various types of cancers [2, 8–15] in different localizations.

PD-L1 is a 40-kDa transmembrane protein (also known as B7-H1 or CD274) and is one of two ligands of the co-inhibitory programmed death receptor 1 (PD-1), expressed on activated immune cell types and involved in maintaining peripheral and central immune cell tolerance [16, 17]. It is mainly detected using immunohistochemistry protocols whose evaluation is difficult even for experienced pathologists and that still need validation [18, 19]. This protein overexpression in malignant cells has been linked to worse prognosis and resistance to anti-cancer therapies [2]. It can be expressed as membrane bound or in a soluble form present in peripheral blood in patients with solid tumors [20]. Also, it is recognized that therapies against PD-L1 result good in non small-cell lung cancer (NSCLC) and other carcinoma patients, their effectiveness depending upon PD-L1 expression. Therefore, analysis of PD-L1 levels is employed for treatment decisions related to these therapies [16, 21–26]. Moreover, it has been reported that serum levels of soluble PD-L1 can be used as non-invasive biomarker to evaluate malignancy of triple-negative breast cancer (TNBC) and pancreatic carcinoma and to predict chemotherapy response in cancer patients [27, 28].

HIF-1α, a transcription factor involved in tumor growth and metastasis by regulating genes involved in response to hypoxia, has been found to be overexpressed in several human cancers and directly associated with increased cancer patient mortality.

Accordingly, due to the endogenous levels of PD-L1 and HIF-1α having been found to be increased and correlated in a wide variety of cancers [9, 14, 29, 30], their single as well as their simultaneous determination would allow a more accurate control of the disease stage and the efficiency of therapies.

Common methods for the determination of PD-L1 and HIF-1α are Western blot [3, 4, 11, 13, 14], ELISA [6], qRT-PCR [3, 4, 13, 14], immunofluorescence staining [14], and immunohistochemistry [2, 8, 9, 11, 12]. These methods are laborious, complex, involve long test times, and are usually limited to centralized environments, requiring highly qualified personnel [31, 32]. To overcome these limitations, electrochemical immunosensors based on the use of magnetic microparticles (MBs) as support for the implementation of bioassays, and of screen-printed electrodes to carry out electrochemical detection, are a promising alternative [33–35]. These immunosensors combine the unique advantages provided by MBs, the high sensitivity and selectivity inherent to immunorecognition events; the low cost; easy handling; simple instrumentation, with ability for miniaturization; easy integration into portable platforms; and the feasibility for multiplexing of electrochemical detection [36]. However, despite the clinical relevance of PD-L1 and HIF-1α, their electrochemical biosensing has been little (HIF-1α [37, 38]) or never explored (PD-L1).

Accordingly, this work reports the development of the first electrochemical immunosensor for the determination of PD-L1. The biosensor involves the use of carboxylic MBs for capturing the target analyte and further labeling with horseradish peroxidase (HRP) followed by amperometric detection at disposable screen-printed carbon electrodes (SPCEs) using the hydroquinone/hydrogen peroxide (HQ/H_2O_2) system. The newly developed electrochemical PD-L1 immunosensor was applied to the determination of this protein in serum samples from breast cancer (BC) patients and lysates of cancer cells grown in normoxia or hypoxia or isogenic pairs with different metastatic potential. In addition, a disposable immunoplatform was prepared to accomplish the simultaneous determination of PD-L1 and HIF-1α, by profiting the availability of the HIF-1α amperometric immunosensor recently developed by our group [38].

Experimental section

Apparatus and electrodes

Amperometric measurements were made using a CHI1140A (CH Instruments, Inc.) potentiostat controlled by the CHI1140A software and a multichannel potentiostat (model 1030B, CH Instruments, Inc.) controlled by the CHI1030B software. Spectrophotometric measurements were performed with a Magellan V 7.1 (TECAN) ELISA plate reader. Single (SPCEs, DRP-110) and dual (SPdCEs, DRP-C1110) screen-printed carbon electrodes and their specific connector cables (DRP-CAC and DRP-BICAC, respectively) were purchased from Metrohm-DropSens S.L. Homemade polymethylmethacrylate (PMMA) casings with one or two embedded neodymium magnets (AIMAN GZ) were employed for the reproducible magnetic capture of the modified MBs on the working electrode (WE) surfaces of the SPCEs and SPdCEs, respectively. All measurements were carried out at room temperature.

Other used instruments were a vortex (Velp Scientifica) to ensure homogenization of the solutions, a BioSan TS-100 incubator shaker with temperature control (Thermo) for MB incubation under stirring conditions, a magnetic separator DynaMag®2 (Invitrogen–Thermo Fisher Scientific), a magnetic stirrer (Inbea S.L.) and a basic pHmeter (Basic 20+, Crison). Digital rocking SHAKER S-4 (ELMI) and clear polystyrene microplates (R&D Systems, Catalog #DY008) were employed to carry out the ELISA tests.

Reagents and solutions

All the employed reagents were of analytical reagent grade. Carboxylic acid–functionalized magnetic microbeads (HOOC-MBs, 2.7 μm Ø, Dynabeads M-270 carboxylic acid, cat. no. 14305D) were purchased from Invitrogen–Thermo Fisher. Blocker casein solution (BB: phosphate-buffered saline (PBS) solution containing 1.0% w/v purified casein) was acquired from Thermo Fisher Scientific. Sodium chloride (NaCl), potassium chloride (KCl), sodium di-hydrogen phosphate (NaH_2PO_4), di-sodium hydrogen phosphate (Na_2HPO_4), and Tris−HCl were purchased from Scharlab, and 2-(N-morpholino)ethanesulfonic acid (MES) was from Gerbu. N-(3-Dimethylaminopropyl)-N′-ethylcarbodiimide (EDC), N-hydroxysulfosuccinimide (sulfo-NHS), hydroquinone (HQ), hydrogen peroxide (H_2O_2) (30%, w/v), and ethanolamine were acquired from Sigma-Aldrich. Sodium hydroxide (NaOH) was from Labkem and tetramethylbenzidine (TMB) commercial solution was from Thermo Scientific™. 25× wash buffer, 10× reagent diluent, and stop solution (2 N H_2SO_4) were included in the DuoSet ELISA Ancillary Reagent Kit 2 (R&D Systems, Catalog #DY008).

Human HIF-1α standard, mouse anti-human HIF-1α capture antibody, and biotinylated goat anti-human HIF-1α detector antibody were purchased from R&D Systems (DuoSet® ELISA Kit, Catalog #DYC1935). Recombinant human PD-L1 standard, mouse anti-human PD-L1 capture antibody, and biotinylated goat anti-human PD-L1 detector antibody were also components of the Human PD-L1 DuoSet® ELISA Kit (Catalog #DY156). Avi-tag biotinylated recombinant human PD-L1 protein from R&D Systems (Catalog #AVI9049-050) was used for the competitive immunoassay. Streptavidin labeled horseradish peroxidase conjugate (Strep-HRP) was purchased from Roche Diagnostics GmbH (Catalog: 11089153001).

Bovine serum albumin (BSA from GERBU Biotechnik GmbH, ref. 1507.0025), IgG from human serum (ref. I2511) and human hemoglobin (ref. H7379) from Sigma-Aldrich, human serum albumin (SIGMA Life Science, ref. A1653), TNF-α protein (BD Pharmigen, ref. 55,618), recombinant human cadherin-17, (liver-intestine cadherin (CDH-17), transcript variant 1 from OriGene Technologies, Inc., ref. TP720740), human total E-cadherin (R&D Systems, ref. DYC4225), recombinant full length human p53 protein (EMD Millipore Corporation, catalog #14-865), human CD105 (endoglin from R&D Systems, ref. DY1097), interferon gamma, IFN-γ (component of human IFN-γ ELISA MAX™ Deluxe Set from BioLegend®, ref. 430,104), recombinant human fibroblast growth factor receptor 4 (FGFR4 from R&D Systems, ref. DYC685-2) and recombinant human interleukin-13 receptor alpha 2 (IL-13Rα2 from R&D Systems, ref. DY614) were evaluated as potential interfering compounds.

The following buffer solutions, prepared with deionized water from a Milli-pore Milli-Q purification system (18.2 MΩ cm), were employed: 0.025 M MES buffer, pH 5.0; PBS consisting of 0.01 M phosphate buffer solution containing 137 mM NaCl and 2.7 mM KCl, pH 7.4; 0.1 M Tris-HCl buffer, pH 7.2; 0.05 M phosphate buffer, pH 6.0; and 0.1 M phosphate buffer, pH 8.0. Wash buffer (0.05% Tween® 20 in PBS) and reagent diluent (1% BSA in PBS) were used for the ELISA method.

0.1 M HQ and H_2O_2 solutions were both prepared in 0.05 M PB (pH 6.0) just before the electrochemical measurements.

The serum samples, provided by Hospital Universitari de Sant Joan (Tarragona, Spain), after approval of the Institutional Ethical Review Boards and getting written informed consent from patients, were used accomplishing all the ethical issues and relevant guidelines and regulations, and stored at − 80 °C until use.

MCF-7, MDA-MB-436, SK-BR-3, SW480, and SW620 (from the American Type Culture Collection (ATCC) cell repository) and KM12C, KM12SM, and KM12L4a (from I. Fidler's laboratory, MD Anderson Cancer Center, Houston, TX) cells were grown and lysed as described previously [39, 40].

Modification of MBs

The protocol for the determination of HIF-1α protein was described in a previous work [38]. Regarding the determination of PD-L1, two different assay methodologies were tested, sandwich or direct competitive (using an Avi-tag biotinylated protein) formats. Carboxylate magnetic beads (HOOC-MBs) were used in both formats, and therefore, similar protocols for washing, activation of the MBs, immobilization of the capture antibody, and the subsequent blocking of the free residual groups were employed.

A 3 μL aliquot of the commercial HOOC-MB suspension was placed into a 1.5-mL microcentrifuge tube and washed twice for 10 min under continuous shaking and constant temperature (25 °C, 950 rpm) with 50 μL of MES buffer (0.025 M, pH 5.0). Then, the HOOC-MBs were placed in a magnetic separator and concentrated for 3 min before removing the supernatant. This procedure was repeated for all the washing steps. Surface carboxylic groups were activated through incubation with 25 μL of a freshly EDC/sulfo-NHS mixture solution (50 mg mL^{-1} each, prepared in MES buffer) for 35 min (25 °C, 950 rpm). Subsequently, the activated MBs were washed twice with MES buffer and incubated for 10 min (25 °C, 950 rpm) in 25 μL of a 25 μg mL^{-1} solution of the specific PD-L1 capture antibody ($CAb_{PD\text{-}L1}$) for the sandwich configuration, or for 15 min (25 °C, 950 rpm) in 25 μL of a 10 μg mL^{-1} $CAb_{PD\text{-}L1}$ solution for the competitive format. The $CAb_{PD\text{-}L1}$-MBs were then washed twice with MES buffer

and incubated in a 1.0 M ethanolamine solution (prepared in 0.1 M phosphate buffer, pH 8.0) for 1 h (25 °C, 950 rpm) to block the residual activated carboxylic groups. Thereafter, the $CAb_{PD\text{-}L1}$-MBs were washed with 0.1 M Tris-HCl buffer (pH 7.2), twice with PBS, and stored at 4 °C in filtered PBS until their use.

Regarding the sandwich assay format, the $CAb_{PD\text{-}L1}$-MBs complexes were incubated in 25 μL of PD-L1 standard solution (or the sample to analyze) both prepared in PBS for 10 min (25 °C, 950 rpm). After washing twice with BB solution, the modified MBs were incubated with 25 μL of a 0.5 μg mL^{-1} PD-L1 biotinylated detector antibody solution ($bDAb_{PD\text{-}L1}$) prepared in BB solution for 30 min (25 °C, 950 rpm), followed by incubation for 5 min in 25 μL of a 1/10,000 diluted Strep-HRP solution (prepared in BB). The MBs bearing the sandwich immunocomplexes were washed twice with BB and re-suspended in 50 μL of 0.05 M phosphate buffer (pH 6.0) to perform the amperometric measurements.

The competitive assay involved the incubation of the $CAb_{PD\text{-}L1}$-MB complexes in 25 μL of PD-L1 standard solution (in PBS) for 45 min (25 °C, 950 rpm). After a washing step with PBS, they were incubated (10 min, 25 °C, 950 rpm) in 25 μL of 1.0 μg mL^{-1} biotinylated PD-L1 solution prepared in PBS. The modified MBs were further labeled through incubation in 25 μL of a 1/10,000 diluted Strep-HRP solution, prepared in BB, for 30 min. Thereafter, the modified MBs were washed twice with BB and re-suspended in 50 μL of 0.05 M phosphate buffer (pH 6.0).

Regarding the simultaneous determination of PD-L1 and HIF-1α, the optimized conditions for the single determination of PD-L1 were slightly modified to unify the procedure for the dual detection. So, the immobilization time of the $CAb_{PD\text{-}L1}$ onto activated HOOC-MBs was 15 min, and the incubation time of the PD-L1 standard (or the sample) was 1 h. All other conditions remained the same as employed for the single determination. The already reported experimental conditions were used for the determination of HIF-1α [38]. Furthermore, the MBs bearing the sandwich immunocomplexes were re-suspended in 5 μL of 0.05 M phosphate buffer, pH 6.0, because of the smaller area of the SPdCEs working electrodes.

Amperometric measurements

After placing the commercial electrode (SPCE for the single determination of PD-L1 or SPdCE for the simultaneous determination of PD-L1 and HIF-1α) over the appropriate PMMA casing, the suspension of modified MBs was dropped and magnetically captured onto the WE surface of the corresponding screen-printed electrode. After immersing the ensemble SPCE/magnet holding block into an electrochemical cell containing 10 mL of 0.05 M PB (pH 6.0) and 1 mM HQ, amperometric signals were recorded in stirred solutions at − 0.20 V vs. the Ag pseudoreference electrode upon addition of 50 μL of a 0.1 M H_2O_2 solution and waiting until reaching the steady-state cathodic current. All the amperometric data were calculated as the difference between the steady-state and the background currents reached after and before the addition of H_2O_2 (in the presence of HQ), respectively, and expressed as the mean values of three replicates ($\alpha = 0.05$). Error bars provided in the Figures were estimated as the standard deviation of three replicates.

Analysis of biological samples

The sandwich immunosensor developed for the single determination of PD-L1 protein was applied to the analysis of lysates from the breast (MCF-7 cells grown in the absence or in the presence of 150 μM $CoCl_2$ to induce hypoxia conditions and simulate metastatic processes, and SK-BR-3) and colorectal (KM12C, KM12SM, KM12L4a, SW480, and SW620) cancer cells. Moreover, serum samples from two healthy individuals and two patients with two different subtypes of BC were analyzed. In addition, the dual immunosensor was applied to the analysis of lysates of breast and colorectal cancer (CRC) cells (MCF-7 treated with and without $CoCl_2$, MDA-MB-436, KM12C, and KM12L4a).

Both the single and dual determinations of the target proteins in cancer cell lysates were carried out using the standard additions method by adding increasing concentrations of PD-L1 (0.0–2.5 ng mL^{-1} for its single determination and 0.0–1.0 ng mL^{-1} for the dual determination) and HIF-1α (0.0–5.0 ng mL^{-1}) standards in the presence of 0.5 μg of raw cell lysate. The same method was employed for the single determination of PD-L1 in 10 μL of non-diluted blood serum samples.

The obtained results for the determination of PD-L1 in cell lysates using the developed immunosensor were compared with those obtained by means of the ELISA method using the same immunoreagents and sample amount. Thus, the well-microplate was coated with 50 μL per well of the 4 μg mL^{-1} $CAb_{PD\text{-}L1}$ solution prepared in PBS and incubated for 2 h. After triple-washing of each well with 400 μL of wash buffer, a blocking step was accomplished by adding 150 μL of reagent diluent to each well and incubating for 1 h. After three additional washings with 400 μL of wash buffer, incubation with 50 μL of the corresponding PD-L1 standard or cell lysate solution, both prepared in Reagent Diluent, was accomplished in each well for 2 h. Three additional washings were carried out as described above. Then the well-microplate was coated with 50 μL of the 50 ng mL^{-1} $bDAb_{PD\text{-}L1}$ solution in Reagent Diluent and incubated for 2 h. After washing, each well was incubated with 50 μL of 1/1000 Strep-HRP dilution, prepared in Reagent Diluent, for 20 min. Once the last washing was performed, 50 μL of TMB commercial solution was added to each well and incubated for 20 min coating the well-

microplate with aluminum foil to avoid direct light. The color reaction was ended by adding 25 μL of Stop Solution to each well, and the optical density was measured immediately using a microplate reader set at 450 nm. All incubation steps were carried out at room temperature. Endogenous contents of PD-L1 in cell lysates were determined by the standard additions method, adding PD-L1 standard concentrations ranging from 0.0 to 1.0 ng mL^{-1} in the presence of 0.5 μg of raw cell lysate.

Results and discussion

This work reports the first electrochemical immunoplatforms prepared for the determination of PD-L1 as well as the first dual immunoplatform for the determination of PD-L1 and HIF-1α.

Immunoplatform for the single determination of PD-L1

Two different immunoassays, sandwich or direct competitive format, were assayed for the single determination of PD-L1 (Fig. 1). Covalent immobilization of the capture antibody ($CAb_{PD\text{-}L1}$) on the surface-confined carboxylic groups of the MBs was performed by using EDC/sulfo-NHS chemistry, which was followed by a blocking step of the remaining activated sites with ethanolamine. The sandwich assay involved sandwiching of the target PD-L1 with a biotinylated secondary antibody ($bDAb_{PD\text{-}L1}$) labeled with a Strep-HRP polymer (Fig. 1a). In the case of the direct competitive format, the $CAb_{PD\text{-}L1}$ immunocomplexes were incubated in a PD-L1 standard solution, followed by an incubation step in Avi-tag biotinylated PD-L1 (bPD-L1) which was labeled with a Strep-HRP solution (Fig. 1b). Avi-tag biotinylated proteins have shown interesting features in terms of uniform labeling and orientation and equivalent bioactivity to the untagged proteins [41].

Both MBs bearing immunoconjugates were magnetically captured on the surface of SPCEs and the cathodic current was measured at −0.20 V vs the Ag pseudoreference electrode using the H_2O_2/HQ system. The change in the cathodic current was proportional to the concentration of the target protein. It is important to note that no success was found when an indirect competitive format was implemented by immobilizing bPD-L1 on MBs modified with streptavidin (Strep-MBs) or neutravidin (Neu-MBs), and making a limited concentration of bDAb labeled with Strep-HRP, to compete for the recognition of free and MB-immobilized PD-L1.

Optimization of the working variables for the PD-L1 immunosensor

a) Sandwich configuration

The optimization of the involved working conditions was carefully evaluated. Each variable value was selected according to the ratio obtained between the amperometric response measured for 2.5 ng mL^{-1} PD-L1 standard (signal, S) and 0 (blank, B) (signal-to-blank, S/B ratio) at − 0.20 V (vs. the Ag pseudoreference electrode). The tested working variables,

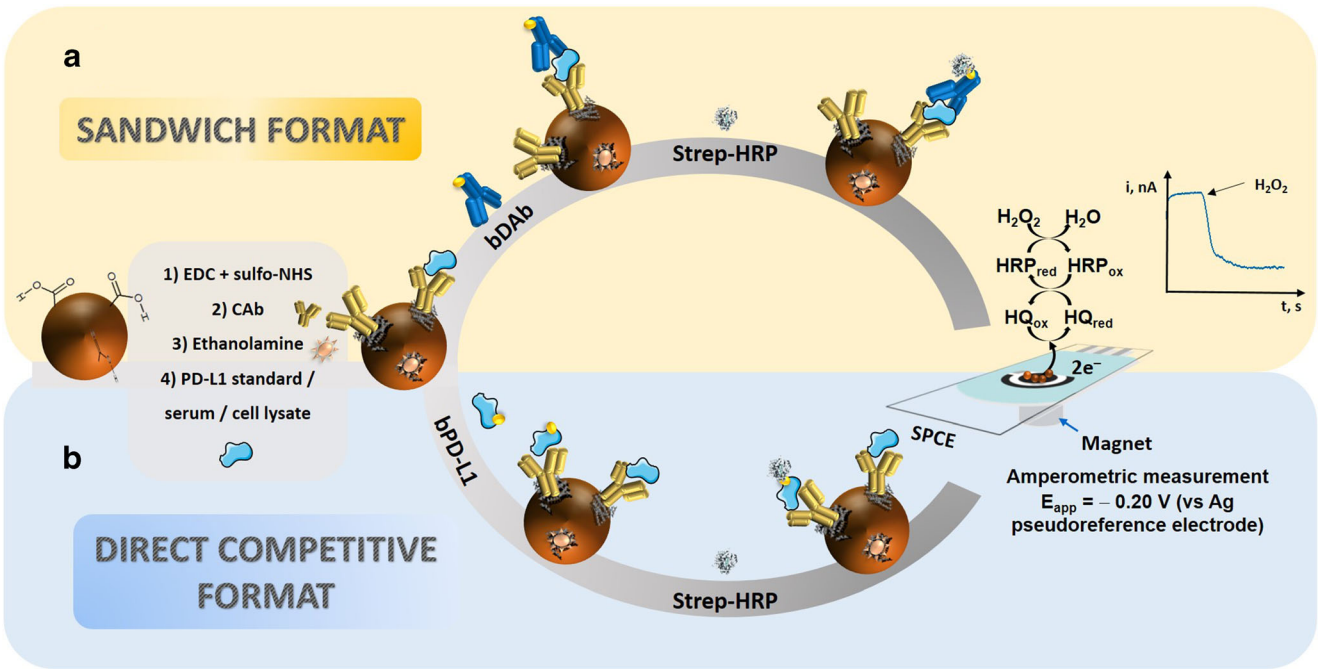

Fig. 1 Schematic display of the steps and reactions involved in sandwich (**a**) and direct competitive (**b**) MB-based immunoassays for the determination of PD-L1

along with the selected values, are summarized in Table S1 and displayed in Fig. S1 in the Supplementary Information (ESM).

Fig. S1a shows that it was not possible to significantly discriminate the presence of PD-L1 at the assayed concentration level in the absence of CAb (bars at 0 in ESM Fig. S1a), in agreement with the rationale of the immunoassay strategy displayed in Fig. 1a). Moreover, the S/B ratio was remarkably large when 25 μg mL^{-1} of $CAb_{PD\text{-}L1}$ (ESM Fig. S1a) were immobilized for 10 min (ESM Fig. S1b), reaching a leveled specific current for larger $CAb_{PD\text{-}L1}$ concentrations, probably due to the CAb saturation on the MBs surface. Different 30 min working step-protocols were tested: (A) three sequential incubation steps of the $CAb_{PD\text{-}L1}$-MBs in PD-L1, $bDAb_{PD\text{-}L1}$, and Strep-HRP solutions, respectively; (B) two sequential incubation steps in PD-L1 standard solution followed by incubating in a solution containing both $bDAb_{PD\text{-}L1}$ and Strep-HRP; (C) two sequential incubations in a PD-L1 and $bDAb_{PD\text{-}L1}$ mixture solution and, thereafter, in the Strep-HRP solution; (D) a single incubation in a mixture solution containing PD-L1, $bDAb_{PD\text{-}L1}$, and Strep-HRP solution. As it can be seen in Fig. S1c, the 3-step working protocol provided by far the best S/B ratio (ESM Fig. S1c, bars A), probably due to agglutination phenomena that occur when working with immunoreagents mixtures or to the worse immunological recognition of the target analyte by the $bDAb_{PD\text{-}L1}$ once labeled with Strep-HRP. Thus, protocol A was selected for further work. The influence of the incubation time with PD-L1, depicted in Fig. S1d (see ESM), showed that a large S/B ratio was reached in only 10 min. The effect of $bDAb_{PD\text{-}L1}$ concentration showed an increase in the S/B with the $bDAb_{PD\text{-}L1}$ concentration up to 0.5 μg mL^{-1}, and a dramatic decrease for larger concentrations possibly due to agglutination phenomena in a homogeneous solution that favored non-specific adsorptions and impaired the specific recognition (ESM Fig. S1e). Moreover, after 30 min of incubation in a 0.5 μg mL^{-1} $bDAb_{PD\text{-}L1}$ solution, the S/B ratio did no increase very much (ESM Fig. S1f); therefore, this time was selected for further studies. Finally, the dilution and incubation time with the Strep-HRP solution showed large S/B ratios for a 1/10,000 dilution (ESM Fig. S1g) and a 5 min incubation time (ESM Fig. S1h).

b) Direct competitive configuration

The competitive format (Fig. 1b) implies a decrease in the sensor response with increasing the concentration of analyte. Therefore, the variables affecting the developed PD-L1 immunosensor were optimized by taking as selection criteria the ratio between the current values measured at − 0.20 V (vs. Ag pseudoreference electrode) in the absence (B) and in the presence of 250 ng mL^{-1} PD-L1 (S) (B/S ratio). The obtained results are summarized in Table S2 and depicted in Fig. S2 in the ESM.

The B/S ratio slightly increased with the concentration of immobilized $CAb_{PD\text{-}L1}$ up to 10.0 μg mL^{-1} (ESM Fig. S2a) and for 15 min incubation (ESM Fig. S2b). Similarly, with bPD-L1 concentration up to 1.0 μg mL^{-1} (ESM Fig. S2e). In both cases, the ratio decreased for larger concentrations, confirming that the use of large concentrations of CAb and bPD-L1 hindered sensitivity as they required a larger target concentration to provide an efficient competition. As it is shown in Fig. S2c (see ESM), the discrimination was not possible when the competition was performed in a single step (by incubating the CAb-MBs in a mixture solution containing PD-L1 and bPD-L1). Moreover, better B/S ratios were obtained for an incubation time in PD-L1 standard solution of 45 min (ESM Fig. S2d) and of 10 min for the competition in bPD-L1 solution (ESM Fig. S2f). In addition, Fig. S2g and h (see ESM) show that better B/S ratios were found for incubation in a 1/10,000 solution of Strep-HRP for 30 min to make the enzymatic labeling.

Analytical characteristics

The calibration plot constructed under the optimized working conditions for the amperometric determination of PD-L1 using the sandwich format immunosensor is displayed in Fig. 2a with a linear range ($r^2 = 0.998$) between 240 and 5000 pg mL^{-1} fitting into the equation: $-i$ (nA) = (260 ± 10) [PD-L1] (nA ng^{-1} mL) + (100 ± 30) (nA). Real amperometric traces recorded for the indicated concentrations are displayed in Fig. 2a(ii). According to the $3 \times s_b/m$ criterion, where s_b was estimated as the standard deviation for 10 measurements recorded in the absence of PD-L1 and m is the slope of the linear calibration plot, a limit of detection (LOD) of 71 pg mL^{-1} was obtained. A relative standard deviation (RSD) value of 2.2%, was calculated from the amperometric responses for 2.5 ng mL^{-1} PD-L1 measured with 10 different MB-sandwich-based immunoplatforms prepared in the same manner, thus indicating the excellent reproducibility of the protocols involved in the preparation of the immunosensor.

Regarding the immunosensor prepared using the direct competitive assay, the calibration plot for PD-L1 and representative real amperometric traces are displayed in Fig. 2b). As expected for a competitive assay, the larger the target concentration the lower the amperometric response due to the lower concentration of bPD-L1 and consequently of Strep-HRP attached to the MBs. The experimental data were fitted to a four-parameter non-linear logistic model, known as Hill's equation, according to the expression:

$$y = i_{\min} + \frac{(i_{\max} - i_{\min})}{1 + \left(\frac{x}{IC_{50}}\right)^{-p}}$$

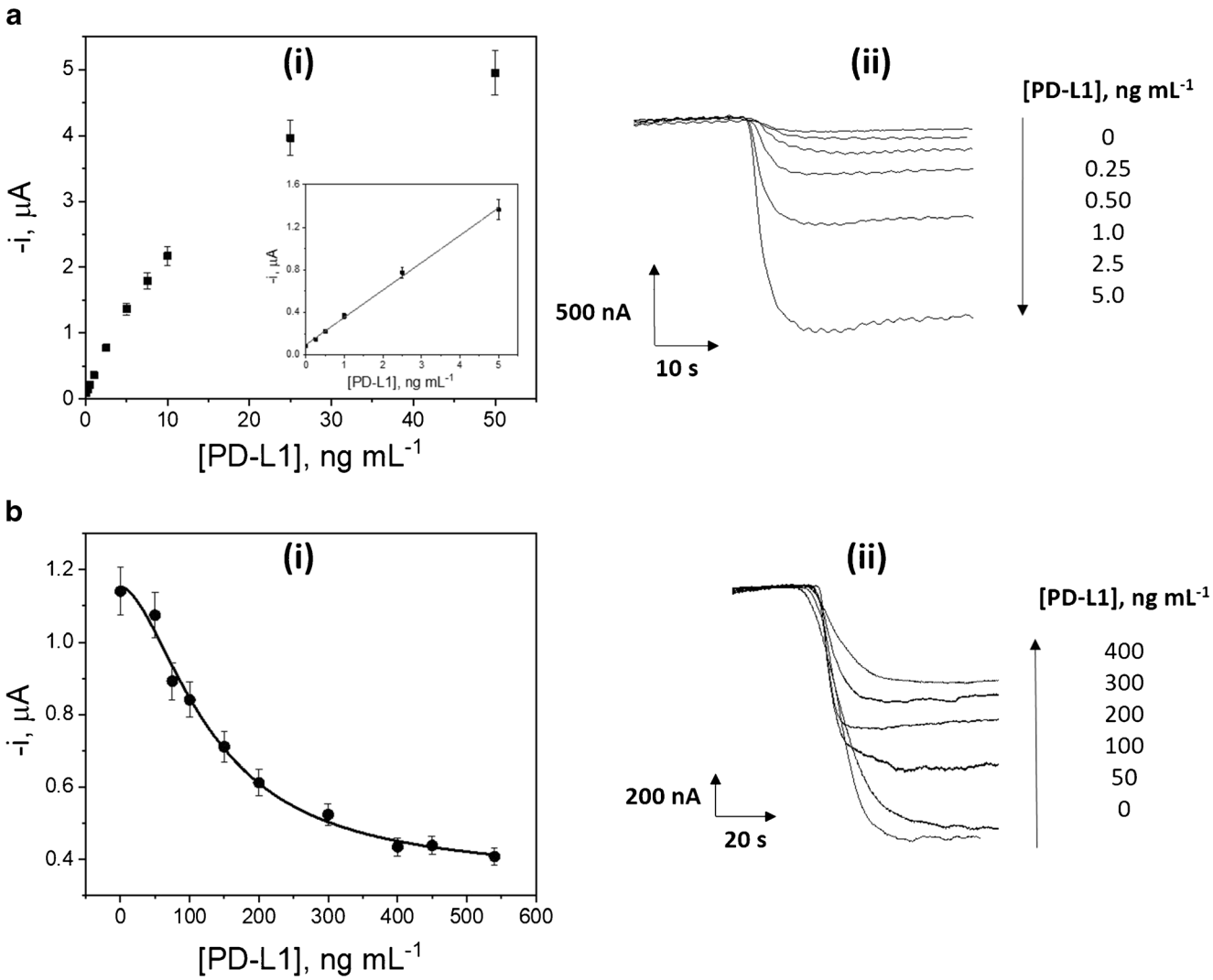

Fig. 2 Calibration curve (i) and amperometric traces (ii) recorded for the amperometric determination of PD-L1 using the developed immunosensors using sandwich (**a**) and direct competitive (**b**) configurations

where i_{max} is the maximum amperometric response in the absence of analyte, i_{min} is the asymptotic minimum current, IC_{50} is the analyte concentration at the inflection point (concentration giving 50% inhibition of i_{max}), and p is the slope at the steepest part of the curve also known as Hill slope [42, 43]. An IC_{50} value of 130 ng mL^{-1} was obtained. The dynamic range from 59 ng mL^{-1} to 289 ng mL^{-1} was calculated as the analyte concentration interval for which the amperometric signal was between 20% and 80% of the maximum signal. In addition, a LOD of 37 ng mL^{-1} was achieved, which was calculated as the analyte concentration for which the maximum amperometric signal was reduced by 10%. It is important to note the considerably lower sensitivity achieved with this competitive format despite the use of an Avi-tag biotinylated recombinant protein (bPD-L1) which provides unique advantages in terms of uniform labeling. Indeed, biotinylation only occurs on the single lysine residue in the Avi-tag, thus allowing its uniform labeling with Strep-HRP, and providing equivalent bioreactivity to that of the untagged protein because the restriction of biotinylation to the Avi-tag keeps unchanged the rest of the protein. In fact, this equivalent bioreactivity of PD-L1 and bPD-L1 may be partly responsible for not obtaining better sensitivity in the competitive format, which would suggest that the use of Avi-tag reagents in competitive formats does not seem to be advantageous over those biotinylated in a conventional way. An RSD value of 5.8% was calculated from the amperometric responses for 100 ng mL^{-1} PD-L1 provided by 10 different immunosensors constructed following the same protocol and prepared on the same day, showing the acceptable reproducibility of the protocols involved in the preparation and the electrochemical transduction with the developed competitive PD-L1 immunoplatforms.

The analytical features achieved with the direct competitive assay are not suitable for the determination of PD-L1 considering the cut-off value in serum of 0.8 ng mL^{-1}, defined by soluble PD-L1 levels determined in a healthy control cohort [44]. In addition, this configuration required a longer time for

the determination (85 vs. 45 min starting from $CAb_{PD\text{-}L1}$-MBs). Therefore, the sandwich assay format, which provided a more than 500 times lower LOD (71 pg mL^{-1} vs. 37 ng mL^{-1}) was selected for further work and utilized for the determination of PD-L1 in real samples.

In this context, the storage stability of the $CAb_{PD\text{-}L1}$-MB conjugates was only evaluated for the sandwich immunoassay methodology (Fig. S3 in the ESM). $CAb_{PD\text{-}L1}$-MBs were stored at 4 °C in 50 μL of filtered PBS and each working day a couple of the prepared bioconjugates were used to prepare the immunoplatforms and measure the amperometric responses in the absence (ESM Fig. S3 white bars, B) or in the presence (ESM Fig. S3 gray bars, S) of 2.5 ng mL^{-1} PD-L1 standards according to the procedure described in *Sections Modification of MBs* and *Amperometric measurements*. Fig. S3 shows the control chart constructed by setting as central value the mean value of the S/B ratios measured with 10 different immunosensors the first day of the study (day 0 in ESM Fig. S3) and ± 3× the standard deviation of this value as the upper and lower control limits. As it can be observed, the stored $CAb_{PD\text{-}L1}$-MB conjugates provided S/B ratios inside the control limits for at least 39 days, which support the possibility of undertaking the determination in just 45 min.

PD-L1 protein has been determined in human serum and cancer cells using colorimetric [45], fluorimetric [46], immunoimaging [47], and near-infrared (NIR) [48] techniques. Moreover, several methodologies have been proposed for the determination of PD-L1+ exosomes employing either optical [49–51] or electrochemical detection [52]. These methodologies provide high sensitivity but they need relatively expensive, hardly portable, and miniaturizable instrumentation, and require much longer assay times than that of the developed immunosensor (45 min). However, there are available several commercial ELISA kits for the determination of PD-L1 with LODs ranging between 0.6 and 154 pg mL^{-1}, which are similar or even smaller than that achieved with the sandwich-based immunosensor (71 pg mL^{-1}). Nevertheless, it is important to note that the developed first electrochemical immunosensor described so far for PD-L1, exhibits a sensitivity, which is adequate for clinical purposes. In addition, it requires shorter assay times (45 min vs. 90 min to 5 h for available ELISA kits) and cheaper instrumentation easy to miniaturize and portable, making its use possible at the point of attention. Furthermore, as it is shown in the following sections, unlike the ELISA methodology, the electrochemical immunosensing strategy is compatible with the simultaneous determination of different biomarkers.

Selectivity

The selectivity of the sandwich immunoplatform was checked by comparing the amperometric responses measured for 0.0 and 2.5 ng mL^{-1} PD-L1 solutions prepared in the absence and in the presence of other proteins and tumor biomarkers found in serum such as human IgG, Hb, HSA, BSA, TNF-α, CDH-17, E-CDH, HIF-1α, endoglin, IFN-γ, FGFR4, IL-13Rα2, and human p53.

Figure 3 shows as no significant differences were apparent in the presence of BSA (bars 4), TNF-α (bars 5), CDH-17 (bars 6), E-CDH (bars 7), HIF-α (bars 8), endoglin (bars 9), and p53 (bars 13). Slightly different responses were found in the presence of IFN-γ (bars 10), FGFR4 (bars 11), and IL-13Rα2 (bars 12). Despite this, all the calculated S/B ratios remained inside the control limits set at ±3 times the standard

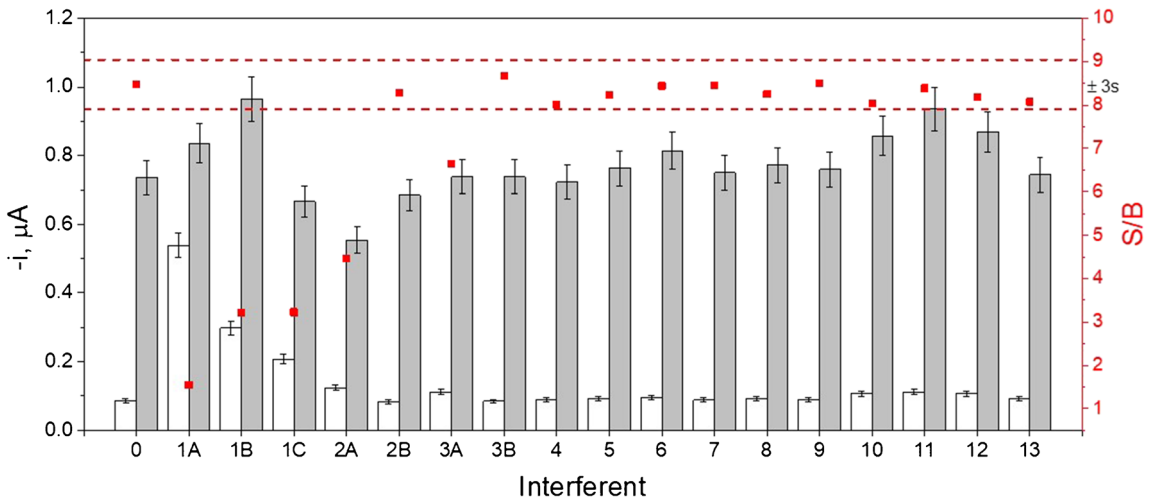

Fig. 3 Amperometric signals measured with the PD-L1 immunosensor prepared using the sandwich configuration for 0.0 (white bars, B) and 2.5 (gray bars, S) ng mL^{-1} PD-L1 (and the corresponding S/B ratio, red squares) prepared without (0) or with potentially interfering compounds: 1.0 mg mL^{-1} human IgG (1A), 0.1 mg mL^{-1} human IgG (1B), 0.01 mg mL^{-1} human IgG (1C), 5.0 mg mL^{-1} Hb (2A), 0.5 mg mL^{-1} Hb (2B), 50.0 mg mL^{-1} HSA (3A), 5.0 mg mL^{-1} HSA (3B), 5.0 mg mL^{-1} BSA (4), 10 ng mL^{-1} TNF-α (5), 500 ng mL^{-1} CDH-17 (6), 10 ng mL^{-1} E-CDH (7), 460 pg mL^{-1} HIF-α (8), 10 ng mL^{-1} endoglin (9), 50 pg mL^{-1} IFN-γ (10), 1.0 ng mL^{-1} FGFR4 (11), 50 ng mL^{-1} IL-13Rα2 (12), and 200 ng mL^{-1} human p53 (13)

deviation of the S/B ratio calculated for PD-L1 standards prepared in the absence of interferent (bars 0).

However, the presence of IgG (Fig. 3, bars 1A–1C), hemoglobin (Fig. 3, bars 2A and 2B), and HSA (Fig. 3, bars 3A and 3B) at different concentrations did affect notably the amperometric measurements. The interference observed in the presence of human IgG can be related to the presence of circulating human antibodies reactive with animal proteins (human anti-animal antibodies, HAAA), which are typically IgGs and recognize epitopes on the Fc portion of foreign immunoglobulins [53]. It is worth mentioning that there are some commercially available solutions to eliminate this widely reported human IgG interference in sandwich immunoassays [54]. The observed interference in the presence of Hb (Fig. 3, bars 2A) can be attributed to its peroxidase activity [55]. Nevertheless, no significant interference occurred when Hb was present at a 10 times lower concentration (Fig. 3, bars 2B). In this sense, it is important to note that the concentration of Hb in the plasma of human individuals is within the 1.6–5.8 μg mL^{-1} range, whose upper limit is more than 800 times lower than the concentration assayed (0.5 mg mL^{-1}; Fig. 3, bars 2B) [56]. Regarding HSA, it is known that unless highly purified, it can contain IgGs with a wide range of specificities that can disturb the assay. HSA interference has been described for other sandwich immunoassays for concentrations above 5 mg mL^{-1} [57]. However, no apparent interference was found when this HSA concentration was tested (Fig. 3, bars 3B). As it is shown in the next section, these potential interferences did not hinder the successful application of the developed immunosensor for the determination of PD-L1 in the analyzed biological samples.

In addition, the supplier of the $CAb_{PD\text{-}L1}$ and $bDAb_{PD\text{-}L1}$ used for implementing the sandwich immunosensor claimed no potential cross-reactivity with B7-1/Fc Chimera, B7-2/Fc Chimera, B7-H2/Fc Chimera, B7-H3, B7-H4, B7-H6/Fc Chimera, PD-L2/Fc Chimera, recombinant mouse B7-H1/Fc Chimera, recombinant rat B7-1/Fc Chimera and recombinant human PD-1/Fc Chimera at concentration levels lower than 50 ng mL^{-1}.

Application to the determination of PD-L1 in serum samples and cell lysates

The developed bioplatform was applied to the determination of PD-L1 in serum samples from healthy individuals and BC patients, as well as in lysates of BC cells grown under normal or hypoxic conditions and isogenic pairs of CRC cells with different metastatic potential.

Considering the presence of matrix effect in serum samples and the low amount of PD-L1 in the cell lysates (no matrix effect was observed for lysates), the determinations were carried out by applying the standard additions method which involved the addition of increasing concentrations of PD-L1 standards in the range of 0.0 to 2.5 ng mL^{-1} to 10 μL of raw undiluted serum or 0.5 μg cell lysate.

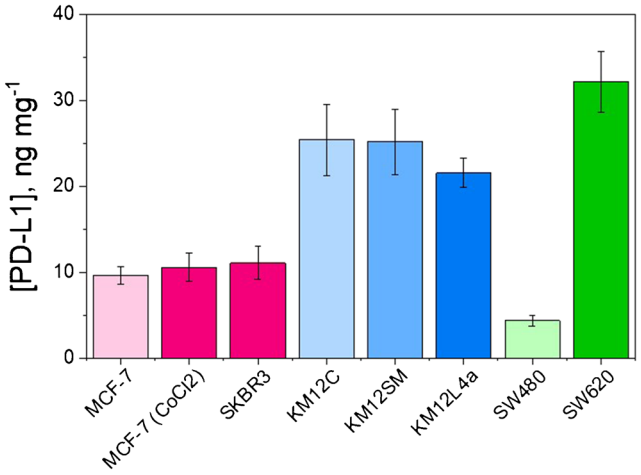

Fig. 4 PD-L1 concentrations determined in cell lysates with the developed immunoplatform

The results provided by the immunosensor in the serum samples were 915 and 950 pg mL^{-1} for the two healthy individuals and 1060 and 1759 pg mL^{-1} for BC patients diagnosed with HER2- and HER2+ subtypes, respectively. The limited availability of these samples did not allow making replicas or analyzing them by the ELISA methodology. Although scarce quantitative data for PD-L1 have been reported in the literature, the remarkable higher PD-L1 concentration found in the serum of the HER2+ patient compared with the HER2- one, agrees well with other reports showing a larger proportion of PD-L1 in the HER2+ than in the HER2- subtype (15 vs 1.3%) [58].

The results obtained in the analysis of cell lysates are displayed in Fig. 4 and summarized in Table 1. The quantitative data agree with the low expression level of PD-L1 measured by flow cytometry in the MCF-7, SKBR3, and SW480 cells [59] and with the reported increased expression during metastasis in CRC [60, 61]. This latter effect can be clearly visualized in the

Table 1 Concentrations of PD-L1 provided by the developed immunoplatform in the different lysates analyzed

Cell type		[PD-L1], ng mg^{-1}*		t_{exp}
		Biosensor	ELISA	
BC	MCF-7	10 ± 1	10 ± 1	0.674
	MCF-7 ($CoCl_2$)	11 ± 2	12 ± 4	0.002
	SKBR3	11 ± 2	13 ± 2	1.747
CRC	KM12C	25 ± 4	24 ± 5	0.544
	KM12SM	25 ± 4	29 ± 3	0.146
	KM12L4a	22 ± 2	24 ± 3	0.218
	SW480	4.4 ± 0.6	6 ± 1	2.740
	SW620	32 ± 4	24 ± 5	1.992

*Mean value ± $ts/\sqrt{n}$; $n = 3$; $\alpha = 0.05$

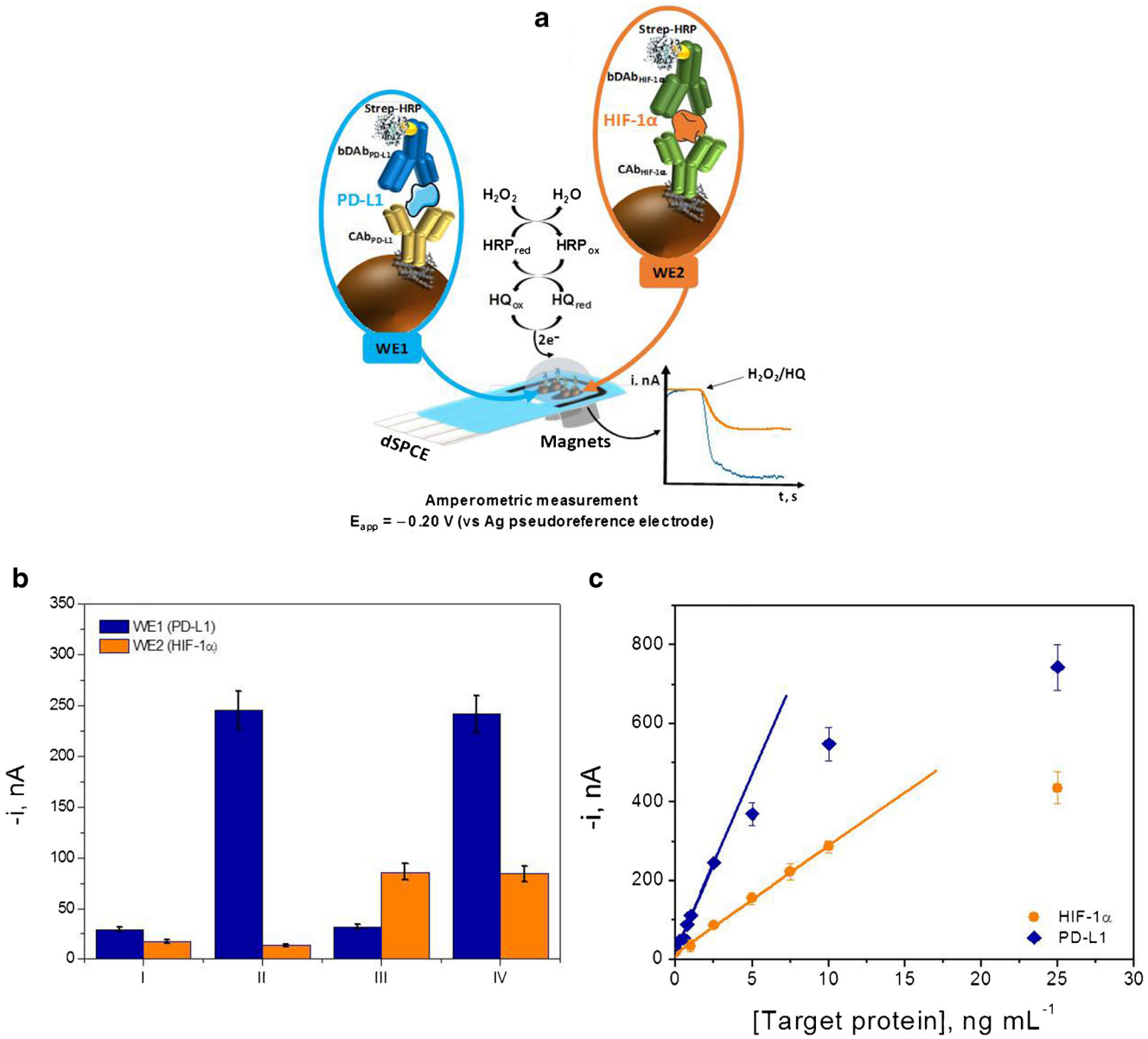

Fig. 5 **a** Scheme and reactions involved in the dual amperometric immunoplatform developed for the simultaneous determination of HIF-1α and PD-L1. **b** Amperometric measurements performed with the dual immunoplatform (WE1: PD-L1, blue bars and WE2: HIF-1α, orange bars) for standard mixtures containing: (I) 0 ng mL^{-1} of both biomarkers; (II) 2.5 ng mL^{-1} PD-L1 and 0 ng mL^{-1} HIF-1α; (III) 0 ng mL^{-1} PD-L1 and 2.5 ng mL^{-1} HIF-1α; and (IV) 2.5 ng mL^{-1} PD-L1 and 2.5 ng mL^{-1} HIF-1α (V). **c** Calibration curves obtained for the amperometric determination of HIF-1α (orange) and PD-L1 (blue) standards

significantly larger expression found in SW620 cells (lymph node metastasis) compared with SW480 cells (isogenic line with the same genetic background as SW620 but without metastatic capacity). However, the similar expression found in isogenic pairs of KM12 with different metastatic capabilities may be due to the heterogeneity of expression in different cell lines. The difficulty to validate methods for the determination of PD-L1 has been attributed to intra-tumor and inter-tumor heterogeneity, as well as low PD-L1 expression for some patients or expression changes especially after chemotherapy [16, 20, 62, 63]. Importantly, Table 1 shows that no significant differences were observed between the results obtained with the developed immunoplatform and the conventional ELISA methodology (t_{exp} values lower that t_{tab} of 2.776, and slope and intercept values of the immunosensor vs. ELISA results plot of 0.8 ± 0.3 and 4 ± 6, respectively).

Simultaneous determination of PD-L1 and HIF-1α

Due to the mentioned high interest for the simultaneous monitoring of PD-L1 and HIF-1α, we have developed a dual immunoplatform for the amperometric determination of both

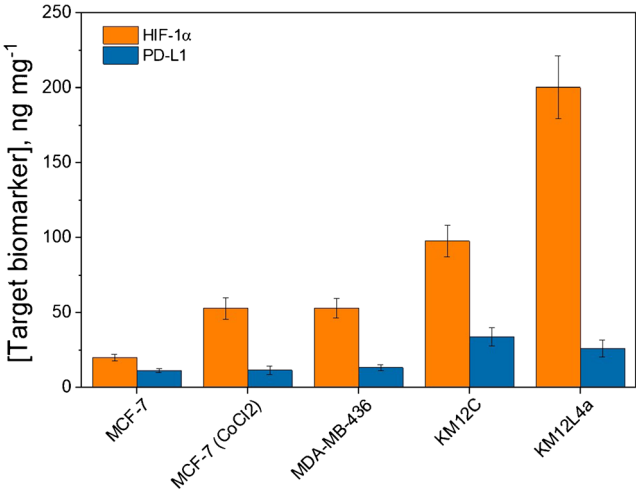

Fig. 6 Target biomarkers concentrations provided by the dual immunoplatforms in the analyzed cellular lysates

biomarkers. The immunoplatform used MBs and SPdCEs and involved electrochemical sandwich-type configurations with bDAbs conjugated with Strep-HRP (Fig. 5a).

The optimized experimental conditions for the single determination of both biomarkers were slightly modified as indicated in "Modification of MBs" to match the developed individual strategies and with a minimal deterioration of sensitivity. The potential cross-talking between the two adjacent working electrodes of the SPdCE was evaluated by comparing the amperometric measurements recorded with both WEs for mixture solutions containing different concentrations of PD-L1 and HIF-1α standards. Figure 5b shows as no apparent cross-talking occurred due to the presence of the non-target biomarker in the adjacent electrode surface. Blue bars displaying the currents recorded with the WE1 in experiments I and III, and orange bars in experiments I and II (WE2) were not significantly different, thus demonstrating the feasibility of the dual immunoplatform for the simultaneous determination of both biomarkers.

The calibration curves for the simultaneous amperometric determination of PD-L1 and HIF-1α are displayed in Fig. 5c. The linear range for PD-L1 extended from 290 to 2500 pg mL^{-1} ($r^2 = 0.994$), fitting the equation $-i$ (nA) = (90 ± 10) [PD-L1] (nA mL ng^{-1}) + (20 ± 10) (nA). The calibration plot for HIF-1α was linear over the 930–10,000 pg mL^{-1} concentration range ($r^2 = 0.998$) fitting the equation $-i$ (nA) = (28 ± 2) [HIF-1α] (nA mL ng^{-1}) + (14 ± 9) (nA). The LOD values, calculated according to the same criterion indicated in *Section Analytical characteristics Section 3.1.2.*) were 86 and 279 pg mL^{-1} for PD-L1 and HIF-1α, respectively. It is important to note that, as expected, these LOD values are slightly higher than those obtained with the single immunosensors (71 and 76 pg mL^{-1} for PD-L1 and HIF-1α, respectively), due to the smaller working electrode surface area of the dual electrodes compared with the single electrodes (6.3 vs. 12.6 mm^2). Nevertheless, the LODs are still considerably lower than the cut-off values established in serum for both target proteins (460 and 800 pg mL^{-1} for HIF-1α [64] and PD-L1 [44], respectively) to discriminate between healthy individuals and cancer patients. The amperometric responses measured for 1.0 ng mL^{-1} PD-L1 and 5.0 ng mL^{-1} HIF-1α with ten different dual immunoplatforms provided RSD values of 2.6 and 3.1% respectively, thus confirming the reproducibility of the protocols used in the preparation and the transduction of the dual immunoplatform. Importantly, to date, no electrochemical platform had been reported in the literature for the simultaneous determination of PD-L1 and HIF-1α.

Application to the simultaneous determination of both hypoxia-related biomarkers in cell lysates

The dual bioplatform was applied to the determination of HIF-1α and PD-L1 in breast and colon cancer cell lysates. As in the case of the single determinations, the standard additions method was used with increasing concentrations of HIF-1α (0.0–1.0 ng mL^{-1}) and PD-L1 (0.0–5.0 ng mL^{-1}) standards to 0.5 μg of each analyzed lysate.

Figure 6 and Table 2 show a higher expression of both target biomarkers in CRC than in BC cells. It is important to note that these results agree with those reported using the ELISA methodology and the biosensors developed for the single determination of PD-L1 and HIF-1 [38]. According to that previously reported [29], a significantly higher HIF-1α content was observed in metastatic cancer cells (MDA-MB-436 and KM12L4a) lysates as well as in the lysates of cells grown in simulated hypoxic conditions (MCF-7 cells treated with $CoCl_2$) compared with their counterparts (non-metastatic KM12C and normoxia-growth MCF-7). Interestingly, these differences were not found in the case of PD-L1, which may be due to several factors such as intratumoral heterogeneity. In

Table 2 Concentration of the target biomarkers, in ng mg^{-1}, obtained with the dual bioplatform in different cell lysates

Target biomarker	MCF-7	MCF-7 ($CoCl_2$)	MDA-MB-436	KM12C	KM12L4a
HIF-1α	20 ± 2	53 ± 7	77 ± 6	100 ± 10	200 ± 20
PD-L1	11 ± 1	12 ± 3	13 ± 2	34 ± 6	26 ± 6

Mean value ± $ts/\sqrt{n}$; $n = 3$; $\alpha = 0.05$

the future, it is intended to deepen these results by analyzing a larger number of samples and comparing them with those provided by a reference method.

Conclusions

An amperometric immunosensor for the determination of the PD-L1 protein cancer biomarker was developed by selecting a sandwich format. The immobilization of specific capture antibody was carried out on activated commercial carboxylate MBs. The immune complex formed after incubating the modified MBs with PD-L1 was recognized with a specific biotinylated detection antibody, which was subsequently labeled with the Strep-HRP conjugate. The modified MBs were magnetically captured on the working electrode of a SPCE and amperometric detection was carried out in the presence of H_2O_2/HQ.

A dual immunoplatform that allowed, for the first time, the simultaneous determination of PD-L1 and HIF-1α, biomarkers of high relevance in tumor hypoxia and metastasis, in just 1 h and 45 min has been also developed. The high reproducibility, selectivity and sensitivity achieved, with LOD values lower than the clinical thresholds, permitted the use of the dual immunoplatform for clinical applications. So, it was employed to the analysis of lysates of breast and colon cancer cells with different metastatic potential by applying the standard additions method and using only 0.5 μg of sample. The reduced analysis time, low cost, easy handling, and miniaturization ability of this dual bioplatform are potentially implementable in devices at the point of care or immediate diagnosis. In this way, more routine controls of the progression of cancer disease and the efficiency of therapies and treatments could be made in outpatient settings or even at home.

Supplementary Information The online version contains supplementary material available at https://doi.org/10.1007/s00216-021-03240-8.

Acknowledgements The financial support of PID2019-103899RB-I00 (Spanish Ministerio de Ciencia e Innovación), RTI2018-096135-B-I00 (Spanish Ministerio de Ciencia, Innovación y Universidades) Research Projects, PI17CIII/00045 and PI20CIII/00019 Grants from the AES-ISCIII Program co-founded by FEDER funds, and the TRANSNANOAVANSENS-CM Program from the Comunidad de Madrid (Grant S2018/NMT-4349) are gratefully acknowledged. C.M.-S.M. acknowledges a predoctoral contract from Universidad Complutense de Madrid. A.M-C. is supported by a FPU predoctoral contract supported by the Spanish Ministerio de Educación, Cultura y Deporte.

Authors' contributions Cristina Muñoz-San Martín: conceptualization, investigation, writing, review, and editing—original draft. Maria Gamella: conceptualization, investigation, writing, review, and editing—original draft. María Pedrero: conceptualization, investigation, writing, review, and editing—original draft. Ana Montero-Calle: investigation, resources, review, and editing—original draft. Víctor Pérez-Ginés: investigation. Rodrigo Barderas: conceptualization, supervision, resources, review, and editing—original draft and funding acquisition. José M. Pingarrón: Review and editing—original draft. Susana Campuzano: conceptualization, supervision, writing, review, and editing—original draft and funding acquisition.

Funding Spanish Ministerio de Ciencia e Innovación (PID2019-103899RB-I00), Spanish Ministerio de Ciencia, Innovación y Universidades (RTI2018–096135-B-I00), AES-ISCIII Program co-founded by FEDER funds (PI17CIII/00045 and PI20CIII/00019 Grants), TRANSNANOAVANSENS-CM Program from the Comunidad de Madrid (Grant S2018/NMT-4349).

Data availability The data that support the findings of this study are available from the corresponding author upon reasonable request.

Declarations

Ethics approval The study was approved by the Ethics Committee (Institutional Review Board) of the Hospital Universitari de Sant Joan de Reus (project code: CEIM 014/2017).

Consent to participate All patients signed a written informed consent according to the declaration of Helsinki.

Consent for publication All authors consent to the publication of the manuscript in Analytical and Bioanalytical Chemistry, should the article be accepted by the Editor-in-chief upon completion of the refereeing process.

Conflicts of interest The authors declare no competing interests.

Disclaimer The funders had no role in the design of the study; in the collection, analyses, or interpretation of data; in the writing of the manuscript; or in the decision to publish the results.

References

1. International Agency for Research on Cancer, World Health Organization, Press Release N° 292, 15 December 2020. https://www.iarc.fr/wp-content/uploads/2020/12/pr292_E.pdf. Accessed 20 Dec 2020.
2. Tawadros AIF, Khalafalla MMM. Expression of programmed death-ligand 1 and hypoxia-inducible factor-1α proteins in endometrial carcinoma. J Cancer Res Ther. 2018;14:1063–9.
3. Barsoum IB, Smallwood CA, Siemens DR, Graham CH. A mechanism of hypoxia-mediated escape from adaptive immunity in cancer cells. Cancer Res. 2014;74:665–74.
4. Noman MZ, Desantis G, Janji B, Hasmim M, Karray S, Dessen P, et al. PD-L1 is a novel direct target of HIF-1α, and its blockade under hypoxia enhanced MDSC-mediated T cell activation. J Exp Med. 2014;211:781–90.
5. Li Y, Patel SP, Roszik J, Qin Y. Hypoxia-driven immunosuppressive metabolites in the tumor microenvironment: new approaches for combinational immunotherapy. Front Immunol. 2018;9:1591. https://doi.org/10.3389/fimmu.2018.01591.
6. Cubillos-Zapata C, Balbás-García C, Avendaño-Ortiz J, Toledano V, Torres M, Almendros I, et al. Age-dependent hypoxia-induced PD-L1 upregulation in patients with obstructive sleep apnoea. Respirology. 2019;24:684–92.

7. Wu Y, Chen W, Xu ZP, Gu W. PD-L1 distribution and perspective for cancer immunotherapy—blockade, knockdown, or inhibition. Front Immunol. 2019;10:2022. https://doi.org/10.3389/fimmu.2019.02022.
8. Chen TC, Wu CT, Wang CP, Hsu W-L, Yang T-L, Lou P-J, et al. Associations among pretreatment tumor necrosis and the expression of HIF-1alpha and PD-L1 in advanced oral squamous cell carcinoma and the prognostic impact thereof. Oral Oncol. 2015;51:1004–10.
9. Chang YL, Yang CY, Lin MW, Wu CT, Yang PC. High co-expression of PD-L1 and HIF-1alpha correlates with tumour necrosis in pulmonary pleomorphic carcinoma. Eur J Cancer. 2016;60:125–35.
10. Dogan HT, Kiran M, Bilgin B, Kiliçarslan A, Sendur MAN, Yalçin B, et al. Prognostic significance of the programmed death ligand 1 expression in clear cell renal cell carcinoma and correlation with the tumor microenvironment and hypoxiainducible factor expression. Diagn Pathol. 2018;13:60. https://doi.org/10.1186/s13000-018-0742-8.
11. Guo R, Li Y, Wang Z, Bai H, Duan J, Wang S, et al. Hypoxia-inducible factor-1α and nuclear factor-κB play important roles in regulating programmed cell death ligand 1 expression by epidermal growth factor receptor mutants in non-small-cell lung cancer cells. Cancer Sci. 2019;110:1665–75.
12. Koh YW, Lee SJ, Han J-H, Haam S, Jung J, Lee HW. PD-L1 protein expression in non-small-cell lung cancer and its relationship with the hypoxia-related signaling pathways: a study based on immunohistochemistry and RNA sequencing data. Lung Cancer. 2019;129:41–7.
13. Zhao Y, Wang X, Wu W, Long H, Huang J, Wang Z, et al. EZH2 regulates PD-L1 expression via HIF-1a in non-small cell lung cancer cells. Biochem Biophys Res Commun. 2019;517:201–9.
14. Zhou L, Cha G, Chen L, Yang C, Xu D, Ge M. HIF1α/PD-L1 axis mediates hypoxia-induced cell apoptosis and tumor progression in follicular thyroid carcinoma. Onco Targets Ther. 2019;12:6461–70.
15. Wen Q, Han T, Wang Z, Jiang S. Role and mechanism of programmed death-ligand 1 in hypoxia-induced liver cancer immune escape (review). Oncol Lett. 2020;19:2595–601.
16. Schott DS, Pizon M, Pachmann U, Pachmann K. Sensitive detection of PD-L1 expression on circulating epithelial tumor cells (CETCs) could be a potential biomarker to select patients for treatment with PD-1/PD-L1 inhibitors in early and metastatic solid tumors. Oncotarget. 2017;8(42):72755–72.
17. Kythreotou A, Siddique A, Mauri FA, Bower M, Pinato DJ. PD-L1. J Clin Pathol. 2018;71:189–94.
18. Oh KS, Mahalingam M. PD-L1 detection—pearls and pitfalls associated with current methodologies focusing on entities relevant to dermatopathology. Am J Dermatopathol. 2019;41:539–65.
19. Stepula E, König M, Wang X-P, Levermann J, Schimming T, Kasimir-Bauer S, et al. Localization of PD-L1 on single cancer cells by iSERS microscopy with Au/Au core/satellite nanoparticles. J Biophotonics. 2019:e201960034. https://doi.org/10.1002/jbio.201960034.
20. Costantini A, Kamga PT, Dumenil C, Chinet T, Emile J-F, Leprieur EG. Plasma biomarkers and immune checkpoint inhibitors in non-small cell lung cancer: new tools for better patient selection? Cancers. 2019;11(9):1269. https://doi.org/10.3390/cancers11091269.
21. Ilie M, Hofman V, Dietel M, Soria J-C, Hofman P. Assessment of the PD-L1 status by immunohistochemistry: challenges and perspectives for therapeutic strategies in lung cancer patients. Virchows Arch. 2016;468:511–25.
22. Grosu HB, Arriola A, Stewart J, Ma J, Bassett R, Hernandez M, et al. PD-L1 detection in histology specimens and matched pleural fluid cell blocks of patients with NSCLC. Respirology. 2019;24:1198–203.
23. Hsieh T-C, Wu JM. Tumor PD-L1 induction by resveratrol/piceatannol may function as a search, enhance, and engage ("SEE") signal to facilitate the elimination of "cold, non-responsive" low PD-L1-expressing tumors by PD-L1 blockade. Int J Mol Sci. 2019;20(23):5969. https://doi.org/10.3390/ijms20235969.
24. Janning M, Kobus F, Babayan A, Wikman H, Velthaus J-L, Bergmann S, et al. Determination of PD-L1 expression in circulating tumor cells of NSCLC patients and correlation with response to PD-1/PD-L1 inhibitors. Cancers. 2019;11(6):835. https://doi.org/10.3390/cancers11060835.
25. Shibel PEE, Abdelhamid HS, Soliman SAM, Gabal SM. Investigation of immunohistochemical expression of programmed death-ligand 1 (PD-L1) in female mammary carcinoma and its correlation with the extent of stromal tumour infiltrating lymphocytes. J Clin Diagn Res. 2019;13(9):EC11–7.
26. Bubendorf L, Conde E, Cappuzzo F, Langfort R, Schildhaus H-U, Votruba J, et al. A noninterventional, multinational study to assess PD-L1 expression in cytological and histological lung cancer specimens. Cancer Cytopathol. 2020;128:928–38.
27. Park H, Bang J-H, Nam A-R, Park JE, Jin MH, Bang Y-J, et al. Prognostic implications of soluble programmed death-ligand 1 and its dynamics during chemotherapy in unresectable pancreatic cancer. Sci Rep. 2019;9:11131. https://doi.org/10.1038/s41598-019-47330-1.
28. Li Y, Cui X, Yang Y-J, Chen Q-Q, Zhong L, Zhang T, et al. Serum sPD-1 and sPD-L1 as biomarkers for evaluating the efficacy of neoadjuvant chemotherapy in triple-negative breast cancer patients. Clin Breast Cancer. 2019;19(5):326–32.
29. Dai X, Pi G, Yang S-L, Chen GG, Liu L-P, Dong H.-H. Association of PD-L1 and HIF-1α coexpression with poor prognosis in hepatocellular carcinoma. Transl Oncol 2018;11:559–566.
30. Chen B, Li L, Li M, Wang X. HIF1A expression correlates with increased tumor immune and stromal signatures and aggressive phenotypes in human cancers. Cell Oncol. 2020;43:877–88.
31. Baraket A, Lee M, Zine N, Sigaud M, Bausells J, Errachid A. A fully integrated electrochemical biosensor platform fabrication process for cytokines detection. Biosens Bioelectron. 2017;93:170–5.
32. Aydin EB, Aydin M, Sezgintürk MK. The development of an ultrasensitive electrochemical immunosensor using a PPyr-NHS functionalized disposable ITO sheet for the detection of interleukin 6 in real human serums. New J Chem. 2020;44:14228–38.
33. Cortina ME, Melli LJ, Roberti M, Mass M, Longinotti G, Tropea S, et al. Electrochemical magnetic microbeads-based biosensor for point-of-care serodiagnosis of infectious diseases. Biosens Bioelectron. 2016;80:24–33.
34. Kudr J, Klejdus B, Adam V, Zitka O. Magnetic solids in electrochemical analysis. TrAC Trends Anal Chem. 2018;98:104–13.
35. Pastucha M, Farka Z, Lacina K, Mikušová Z, Skládal P. Magnetic nanoparticles for smart electrochemical immunoassays: a review on recent developments. Microchim Acta. 2019;186:312. https://doi.org/10.1007/s00604-019-3410-0.
36. Pingarrón JM, Campuzano S, González-Cortés A, Yáñez-Sedeño P. Electrochemical immunosensors for clinical diagnostics. In: Wandelt K, editor. Encyclopedia of interfacial chemistry: surface science and electrochemistry: Elsevier; 2018. p. 156–65.
37. Hussain KK, Gurudatt NG, Mir TA, Shim Y-B. Amperometric sensing of HIF1α expressed in cancer cells and the effect of hypoxic mimicking agents. Biosens Bioelectron. 2016;83:312–8.
38. Muñoz-San Martín C, Gamella M, Pedrero M, Montero-Calle A, Barderas R, Campuzano S, et al. Magnetic beads-based electrochemical immunosensing of HIF-1α, a biomarker of tumoral hypoxia. Sensors Actuators B Chem. 2020;307:127623. https://doi.org/10.1016/j.snb.2019.127623.
39. Torrente-Rodríguez RM, Ruiz-Valdepeñas Montiel V, Campuzano S, Pedrero M, Farchado M, Vargas E, et al. Electrochemical sensor for rapid determination of fibroblast growth factor receptor 4 in raw

cancer cell lysates. PLoS One. 2017;12:e0175056. https://doi.org/10.1371/journal.pone.0175056.
40. Valverde A, Povedano E, Ruiz-Valdepeñas Montiel V, Yáñez-Sedeño P, Garranzo-Asensio M, Barderas R, et al. Electrochemical immunosensor for IL-13 receptor α2 determination and discrimination of metastatic colon cancer cells. Biosens Bioelectron. 2018;117:766–72.
41. Xue H, Bei Y, Zhan Z, Chen X, Xu X, Fu YV. Utilizing biotinylated proteins expressed in yeast to visualize DNA–protein interactions at the single-molecule level. Front Microbiol. 2017;8:2062. https://doi.org/10.3389/fmicb.2017.02062.
42. Escamilla-Gómez V, Campuzano S, Pedrero M, Pingarrón JM. Development of an amperometric immunosensor for the quantification of Staphylococcus aureus using self-assembled monolayer-modified electrodes as immobilization platforms. Electroanalysis. 2007;19:1476–82.
43. Gadagkar SR, Call GB. Computational tools for fitting the Hill equation to dose–response curves. J Pharmacol Toxicol Methods. 2015;71:68–76.
44. Finkelmeier F, Canli O, Tal A, Pleli T, Trojan J, Schmidt M, et al. High levels of the soluble programmed death-ligand (sPD-L1) identify hepatocellular carcinoma patients with a poor prognosis. Eur J Cancer. 2016;59:152–9.
45. Wuethrich A, Rajkumar AR, Shanmugasundaram KB, Reza KK, Dey S, Howard CB, et al. Single droplet detection of immune checkpoints on a multiplexed electrohydrodynamic biosensor. Analyst. 2019;144:6914–21.
46. Yazdian-Robati R, Ramezani M, Khedri M, Ansari N, Abnous K, Taghdisi SM. An aptamer for recognizing the transmembrane protein PDL-1 (programmed death-ligand 1), and its application to fluorometric single cell detection of human ovarian carcinoma cells. Microchim Acta. 2017;184:4029–35.
47. Ou Y-C, Wen X, Johnson CA, Shae D, Ayala OD, Webb JA, et al. Multimodal multiplexed immunoimaging with nanostars to detect multiple immunomarkers and monitor response to immunotherapies. ACS Nano. 2020;14:651–63.
48. Zhang M, Jiang H, Zhang R, Jiang H, Xu H, Pan W, et al. Near-infrared fluorescence-labeled anti-PD-L1-mAb for tumor imaging in human colorectal cancer xenografted mice. J Cell Biochem. 2019;120:10239–47.
49. Liu C, Zeng X, An Z, Yang Y, Eisenbaum M, Gu X, et al. Sensitive detection of exosomal proteins via a compact surface plasmon resonance biosensor for cancer diagnosis. ACS Sens. 2018;3:1471–9.
50. Pang Y, Shi J, Yang X, Wang C, Sun Z, Xiao R. Personalized detection of circling exosomal PD-L1 based on Fe_3O_4@TiO_2 isolation and SERS immunoassay. Biosens Bioelectron. 2020;148:111800. https://doi.org/10.1016/j.bios.2019.111800.
51. He Y, Wu Y, Wang Y, Wang X, Xing S, Li H, et al. Applying CRISPR/Cas13 to construct exosomal PD-L1 ultrasensitive biosensors for dynamic monitoring of tumor progression in immunotherapy. Adv Ther. 2020;3:2000093. https://doi.org/10.1002/adtp.202000093.
52. Cao Y, Wang Y, Yu X, Jiang X, Li G, Zhao J. Identification of programmed death ligand-1 positive exosomes in breast cancer based on DNA amplification-responsive metal-organic frameworks. Biosens Bioelectron. 2020;166:112452. https://doi.org/10.1016/j.bios.2020.112452.
53. Melanson SEF, Tanasijevic MJ, Jarolim P. Cardiac troponin assays: a view from the clinical chemistry laboratory. Circulation. 2007;116:e501–4.
54. Tate J, Ward G. Interferences in immunoassay. Clin Biochem Rev. 2004;25:105–20.
55. Grigorieva DV, Gorudko IV, Sokolov AV, Kosmachevskaya OV, Topunov AF, Buko IV, et al. Measurement of plasma hemoglobin peroxidase activity. Bull Exp Biol Med. 2013;155:118–21.
56. Anderson RL, Chaplin H Jr. Plasma hemoglobin concentration in umbilical cord blood. Am J Dis Child. 1963;105:19–26.
57. Zhao R-N, Feng Z, Zhao Y-N, Jia L-P, Ma R-N, Zhang W, et al. A sensitive electrochemical aptasensor for Mucin 1 detection based on catalytic hairpin assembly coupled with PtPdNPs peroxidase-like activity. Talanta. 2019;200:503–10.
58. Kurozumi S, Inoue K, Matsumoto H, Fujii T, Horiguchi J, Oyama T, et al. Clinicopathological values of PD-L1 expression in HER2-positive breast cancer. Sci Rep. 2019;9:16662. https://doi.org/10.1038/s41598-019-52944-6.
59. Grenga I, Donahue RN, Lepone L, Bame J, Schlom J, Farsaci B. PD-L1 and MHC-I expression in 19 human tumor cell lines and modulation by interferon-gamma treatment. J Immunother Cancer. 2014;2:P102. https://doi.org/10.1186/2051-1426-2-S3-P102.
60. Wang HB, Yao H, Li CS, Liang LX, Zhang Y, Chen YX, et al. Rise of PD-L1 expression during metastasis of colorectal cancer: implications for immunotherapy. J Dig Dis. 2017;18:574–81.
61. Shan T, Chen S, Wu T, Yang Y, Li S, Chen X. PD-L1 expression in colon cancer and its relationship with clinical prognosis. Int J Clin Exp Pathol. 2019;12:1764–9.
62. Kerr KM, Nicolson MC. Non–small cell lung cancer, PD-L1, and the pathologist. Arch Pathol Lab Med. 2016;140:249–54.
63. Rom-Jurek E-M, Kirchhammer N, Ugocsai P, Ortmann O, Wege AK, Brockhoff G. Regulation of programmed death ligand 1 (PD-L1) expression in breast cancer cell lines in vitro and in immunodeficient and humanized tumor mice. Int J Mol Sci. 2018;19(2):563. https://doi.org/10.3390/ijms19020563.
64. Prasad J, Goswami B, Gowda SH, Gupta N, Kumar S, Agarwal K, et al. Does hypoxia-inducible factor-1a (HIF-1a) C1772T polymorphism predict short-term prognosis in patients with oral squamous cell carcinoma (OSCC). J Oral Pathol Med. 2018;47:660–4.